X-621-75-254
PREPRINT

NEUTRAL COMPOSITION GRAVITY WAVES IN THE THERMOSPHERE OBSERVED BY ESRO 4

H. TRINKS
H. G. MAYR

OCTOBER 1975

GSFC

GODDARD SPACE FLIGHT CENTER
GREENBELT, MARYLAND

X-621-75-254

NEUTRAL COMPOSITION GRAVITY WAVES IN THE ERMOSPHERE OBSERVED BY ESRO 4

H. TRINKS*

H. G. MAYR

Laboratory for Planetary Atmosphere

*NAS/NRC Resident Research Associate, on leave from
Physikalisches Institut, Universitaet Bonn, Germany

GODDARD SPACE FLIGHT CENTER
GREENBELT, MARYLAND

NEUTRAL COMPOSITION GRAVITY WAVES IN THE THERMOSPHERE

OBSERVED BY ESRO 4

ABSTRACT

Neutral composition waves with a wave length of about 5000 km and a wave period of about 2.5 hours were observed by ESRO 4 in the altitude region of 250 km. The amplitudes are of the order of 25% for Ar, 15% for N_2, and roughly 10% for He and O at 25° geographic latitude. The Ar and N_2 waves are almost in phase, whereas He is in anti-phase and O is in between. The wave amplitudes are seen to decrease towards lower latitudes suggesting that the composition waves are launched by auroral sources. Simultaneous ground based ionosonde measurements of the F2 layer critical frequency at mid and low latitudes show a wave period consistent with the satellite observations. From the relation between wave length and wave period these waves are identified as gravity waves. The theoretical investigation with a multi-component model shows that diffusion plays a major role in explaining these wave phenomena. The phase and amplitude relation between atmospheric constituents are sensitive to the altitude region in which energy is deposited thus suggesting that Joule heating or soft particle precipitation are the predominant energy sources.

NEUTRAL COMPOSITION GRAVITY WAVES IN THE THERMOSPHERE OBSERVED BY ESRO 4

INTRODUCTION

Since Hines [1960] postulated internal atmospheric gravity waves only a few observations of wave-like structures of the neutral gas density have been published [e.g. Newton et al., 1969; Forbes and Marcos, 1973]. Recently, measurements in the lower and middle thermosphere obtained by satellite borne neutral gas mass spectrometers were reported by Hedin et al., [1974], Proelss and von Zahn [1975] revealing the existence of wave structures in the neutral composition, the "wavelength" ranging between about 30 km and several 100 km. This paper presents neutral composition data obtained by the gas analyzer aboard ESRO 4 during four consecutive perigee passes showing large scale wave structures which are interpreted as gravity waves.

EXPERIMENTAL METHOD

ESRO 4 was a spin-stabilized polar orbiting spacecraft with an inclination of 91°. During the time interval to be discussed here the perigee height was 235 km while the apogee height was about 500 km, thus the height variation within the considered latitude range of 120° was only 80 km. The perigee latitude was about 38° S, the local solar time at perigee was 13:36. The gas analyzer [Trinks and von Zahn, 1975] measured the number densities of the total oxygen content $n(O) + 2\,n(O_2)$, molecular nitrogen $n(N_2)$, helium n(He) and argon n(Ar). The measured oxygen content reflects mainly the atomic oxygen density since the contribution of molecular oxygen becomes negligible under most circumstances above the ESRO 4 perigee.

METHOD OF DATA ANALYSIS

For this study the density data of four orbits obtained between 1:15 and 6:20 UT on 6 March, 1974 within the geographic latitude range 15°N...89°S...75°S were selected. From these data it was apparent that altitude, latitude and local solar time dependence of the density of each atmospheric constituent in most cases exceeded the wave induced structures. Consequently, the variations not associated with wave structures had to be filtered out.

To eliminate the altitude dependence the densities of all constituents except helium were converted into exospheric temperatures using Jacchia's model [Jacchia, 1971]. The latitude and local solar time dependence of the obtained temperatures were filtered out by applying a least square analysis in terms of low order spherical harmonics. The local solar time dependence was included to distinguish both sides of the south pole sampled by ESRO 4. In order to fit only those structures which re unchanged from one pass to the next, the fit for each constituent included the data of all four passes. Thus a temperature fit for O, for N_2 and for Ar was obtained. The exospheric temperature fits were then reconverted into densities using again Jacchia's model. In the case of helium the density data were directly fitted by spherical harmonics since the altitude variations in the height range of 80 km were small. Figure 1 represents the resulting density fits versus geographic latitude; also shown is the latitude dependence of the satellite altitude during the passes considered. In the higher latitude region the neutral composition obviously is disturbed (increased Ar and N_2 density, decreased He

and O density) in response to disturbed geomagnetic conditions; during this time interval a_p changed from 27 to 7.

In order to separate the wave structures the original density data were finally compared with the density fits by computing the ratio $R(\Theta)$ for each constituent and orbit, Θ being the geographic latitude. Since the same fit was used for all passes, the centerlines of the $R(\Theta)$ data were slightly different from unity which was especially true at higher latitudes. Therefore the ratios $R(\Theta)$ were fitted by the spherical harmonics P_0 and P_1 for each constituent and orbit. The old ratios were then divided by the corresponding fit values and replaced by these new ratios. This procedure eliminated the global scale variations from one pass to the other without significantly effecting the wave structures. The results are presented in Figure 2 for Ar, N_2, O and He. In order to emphasize the wave structures with large wavelengths (which are to be investigated in this paper), smoothed curves were hand fitted to the data points neglecting small scale variations.

DISCUSSION

At low and midlatitudes a well pronounced sinusoidal wave structure develops in the case of Ar and N_2 and weaker but still recognizable in the case of O and He. The "wavelength" is of the order of 50° latitude corresponding to about 5000 km which has to be considered as an upper limit of the real wavelength since the satellite's trajectory was not necessarily perpendicular to the wave front. The phases of the N_2 wave show a slight phase difference when compared with the Ar wave, whereas both O and He are almost in antiphase. In the higher latitude region the

large scale wave structure is more difficult to identify because small scale disturbances and waves become predominant. There is a well pronounced localized disturbance between 60° and 70° geographic latitude during pass #1 and somewhat weaker during pass #2 which is of the kind described by Wulf-Mathies et al., [1974] and might define the source region of the observed waves. Small scale wave structures are especially developed during pass #4; note that for this case there is only a slight phase difference between the 3 constituents Ar, N_2 and O, (a corresponding wave structure in He cannot be recognized due to the scatter of data points).

To demonstrate the time development of the wave structure the smoothed curves of all four passes (see Figure 2) are put into one frame in the case of argon (Figure 3). Although it cannot be excluded that there is a longitudinal variation of the wave structure we assume that most of the observed changes from one pass to the next reflect a time development; in the following, this assumption will be strongly supported.

Since we have four consecutive passes showing wave structures with almost the same amplitudes it is possible to fit the 4 data points $R(\Theta_o)$ (see Figure 2) obtained at a fixed latitude Θ_o during all passes by a cosine function versus time t:

$$R(\Theta_o,t) = a \cos(\omega t + \alpha),\ t = t(\Theta_o) \text{ for passes 1-4}$$

The fit in turn yields the amplitude a, the frequency ω, and the phase α for each constituent. In order to reduce the influence from the scatter of the data points especially in the case of He and Ar mean values $R(\Theta_o,t)$ were used including 5 data points $R(\Theta_o \pm \Delta\Theta,t)$ closest to the

selected latitude θ_o. To linearize the fit problem ω was set constant when applying the least mean square fit method. Varying ω by steps the minimum of the standard deviation finally determined the best fit for ω. In the case of Ar (and N_2) a well pronounced minimum of the standard deviation was found for a wave period $2\pi/\omega$ = 140...150 min. For O and He in most cases no clear minimum of the standard deviation could be identified because of the small amplitudes of the O and He wave and the scatter of data points (helium). In Table I the obtained wave parameters are listed for a wave period of 140 and 150 min at different geographic latitudes. At 25°S the Ar wave shows an amplitude of about 25% which is significantly decreasing towards the equator; furthermore a phase difference of π is found between 25°S and the equator, yielding again a "wavelength" of about 50° in latitude. For N_2 the results are almost the same concerning the phase, whereas the amplitude is less by about 40%. For O and He the results from Table I show a phase difference of roughly 0.7π in the case of O and π in the case of He with respect to the Ar wave. The amplitudes are relatively small and become comparable to the standard deviations. (No results are presented at 0° and 12.5°S geographic latitude where the standard deviations exceed the amplitudes).

The waves observed by the ESRO 4 gas analyzer are in good agreement with ionospheric waves as deduced from F2 layer critical frequency data. Figure 4 represents f_oF2 from three Australian and one New Guinean station located at geographic longitudes between ESRO 4 passes #2 and 3 (see Figure 2). Although the time resolution is poor and the fit curves in some cases may be questionable, the overall data clearly exhibit

ionospheric waves with a period of about 2.5 hours. The wavelength turns out to be about 50° in latitude, considering that the ionospheric waves above Brisbane (28°S) and Vanimo (3°S) are almost in antiphase as marked by the dashed line at 15:10 EMT (5:10 UT). The wave maxima, which are presumably associated, are identified by arrows, indicating the progression of a wave towards lower latitudes.

A model for the excitation of composition gravity waves has recently been discussed by Mayr and Volland [1975] where it was shown that wind induced diffusion is significant in producing phase differences between atmospheric constituents. The equations of mass, energy and momentum conservation were solved for a multi-component gas (including N_2, O and He) considering horizontal and vertical diffusion. Time and latitude dependence were separated in terms of Fourier and spherical harmonics; longitudinal and local time variations were ignored. The heat source responsible for exciting these waves was assumed to peak near 140 km due to Joule heating in the auroral zones. The upper and lower boundaries of the model were at 700 and 80 km respectively, presumably removed far enough from the excitation region so that homogeneous boundary conditions are justified. For our interpretation we adopted this model but extended it to include argon.

Adopting the spherical harmonic P_8 corresponding to an average wave length of 5000 km (in accordance with the predominant wave structure in our data) the thermospheric response was evaluated for a series of frequencies. The resulting amplitudes and phases of Tg, O and N_2 are

shown for 250 km in Figure 5. It reveals resonance maxima near 6 x 10^{-4} sec^{-1} (τ = 2.9 hours) indicating that most of the wave energy for the 5000 km wave length is carried by a wave period of 2.9 hours, in reasonable agreement with our observations. Since the physical mechanisms for producing the resonance maximum also led to the dispersion relation in gravity wave theory we identify these waves as gravity waves. The rapid phase transitions near the "resonance frequency" are responsible for the wave propagation as was shown by Mayr and Volland [1975]. By comparison, the phase differences between O and N_2 (and similarly between other constituents) remain relatively constant which makes them particularly useful in comparative studies regarding the excitation source for example.

For P_8 and ω = 6 x 10^{-4} sec^{-1} the amplitude and phase distributions of temperature and composition are shown in Figure 6. The relative amplitudes of the atmospheric constituents are in substantial agreement with the ESRO 4 data at 250 km. The extent to which deviations from diffusive equilibrium are important for N_2, O and He has been discussed by Mayr and Volland [1975]. For Ar the amplitude of the "effective scale height temperature" (defined in Mayr et al. [1974]) exceeds the gas temperature by 70% at 150 km and 30% at 250 km, which contributes significantly to the comparatively large Ar density amplitude. It is apparent from Figure 6 that the phase differences between individual constituents agree qualitatively with the ESRO 4 measurements at 250 km altitude: The difference is small between N_2 and Ar (20°) and largest between Ar and He (110°); the phase difference between Ar and O (60°) is in between.

Apart from the uncertainties in the phase determination of satellite data there are considerable uncertainties in the excitation of composition waves. Momentum sources associated with ion convection, and local time or longitudinal variations could be important. Furthermore, the height structure of the heat source is not well determined, depending on the height distribution of the electron density in the case of Joule heating and depending on the energies of precipitating particles.

Moving the heat input maximum from 140 km (the case discussed earlier) up to 200 km has pronounced effects on the phase relations between atmospheric constituents. This is illustrated in Figure 7 where the phase differences with respect to Ar are shown as a function of height. With the exception of N_2 the Ar-O and Ar-He phase differences are considerably larger for the 200 km than for the 140 km heat source, in better agreement with the ESRO 4 data. From the comparison between the experimental results and the theory we are led to conclude that thermospheric sources, possibly as high in altitude as 200 km, are responsible for the excitation of the observed wave phenomena.

Acknowledgements

One of us (H.T.) is indebted to the National Academy of Sciences/ National Research Council of the U.S.A. for the award of a Post-Doctoral Research Associateship and to Goddard Space Flight Center for hospitality. We want to thank U. von Zahn for his continuous support. The help of K. H. Fricke and U. Laux is appreciated. Thanks is also due to I. Brophy of the World Data Center A for supplying us with ionospheric data used in this study. Part of this research is supported through grant WRK 107 of the Bundesministerium fuer Forschung and Technologie, Bonn.

References

Forbes, F. M., and F. A. Marcos, Thermospheric density variations associated with auroal electrojet activity, J. Geophys. Res., 78, 3841, 1973.

Hedin, A. E., C. A. Reber, D. T. Pelz, and G. R. Carignan, Composition variations in the lower thermosphere observed by the NACE instrument on the AE-C spacecraft, Transactions of the Am. Geophys. Union, 56, 1162, SA100, 1974.

Hines, C. O., Internal atmospheric gravity waves at ionospheric heights, Can. J. Phys., 38, 1441, 1960.

Jacchia, L. G., Revised static models of the thermosphere and exosphere with empirical temperature profiles, Spec. Rep. 332, 113 , Smithson. Astrophys. Observ., Cambridge, Mass., 1971.

Mayr, H. G., and H. Volland, Composition waves in the thermosphere, in press, J. Geophys. Res., 1975.

Mayr, H. G., I. Harris, and N. W. Spencer, Thermospheric 'Temperatures', J. Geophys. Res., 79, 2921, 1974.

Newton, G. P., D. T. Pelz, and H. Volland, Direct in situ measurements of wave propagation in the neutral thermosphere, J. Geophys. Res., 74, 183, 1969.

Proelss, G. W., and U. von Zahn, Large and small scale changes in the disturbed upper atmosphere, paper presented at 18th COSPAR meeting at Varna, Bulgaria, 1975.

Trinks, H., and U. von Zahn, The ESRO 4 gas analyzer, Rev. Sci. Instr. 46, 213, 1975.

Wulf-Mathies, C., P. Blum, and H. Trinks, Local composition changes in the thermosphere at high latitudes during moderate geomagnetic conditions, Space Res., 14, (in press), 1974.

Table I. Period $2\pi/\omega$, amplitude a, and phase α as derived from best fit $R(\theta_o,t) = a \cos(\omega t + \alpha)$ at fixed geographic latitudes θ_o; $R(\theta_o,t)$ as in Fig. 2. Also listed is the minimum standard deviation S.Dev. and the halfwidth $\Delta(2\pi/\omega) = (2\pi/\omega_1) - (2\pi/\omega_2)$, ω_1 and ω_2 correspond to twice the minimum standard deviation (see also text).

θ_o [°S]	Gas	$2\pi/\omega$ [min]	a [%]	α [π]	S.DEV. [%]	$\Delta(2\pi/\omega)$ [min]
25.0	Ar	140	25.3	1.28	2.8	15
		150	24.4	1.11	4.4	
	N_2	140	14.4	1.27	5.2	30
		150	15.0	1.12	3.6	
	O	140	6.3	2.0	5.1	--
		150	7.3	1.84	5.0	
	He	140	7.6	2.16	6.5	--
		150	9.0	2.06	6.0	
12.5	Ar	140	9.0	1.72	1.3	15
		150	9.1	1.64	0.6	
	N_2	140	4.5	1.56	5.7	--
		150	4.5	1.42	5.4	
0	Ar	140	8.8	2.32	2.2	35
		150	7.7	2.15	3.3	

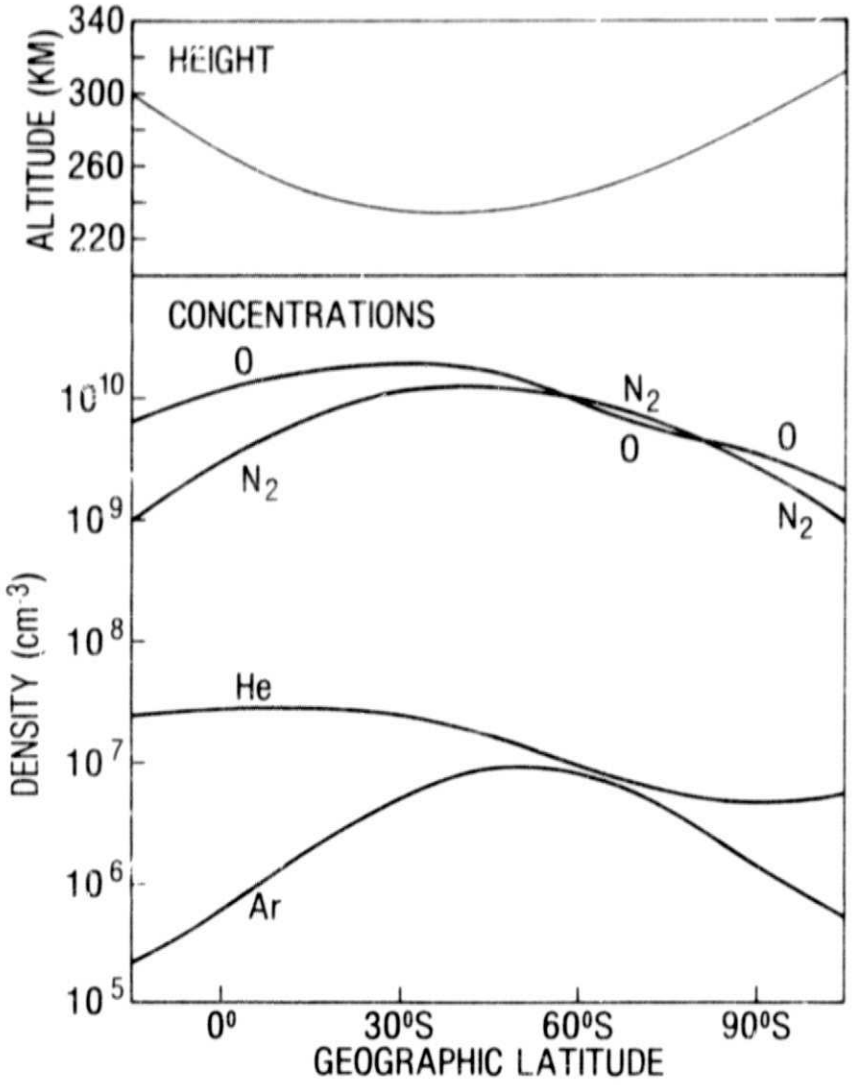

Figure 1: Fits of atomic oxygen, molecular nitrogen, helium and argon number densities obtained during 4 orbits (passes 1-4) between 1:15 and 6:20 UT on 6 March, 1974. The uppermost curve represents the altitude of observation. The local solar time at perigee was 13:36. The density fits are used to make wave structures recognizable (see Fig. 2).

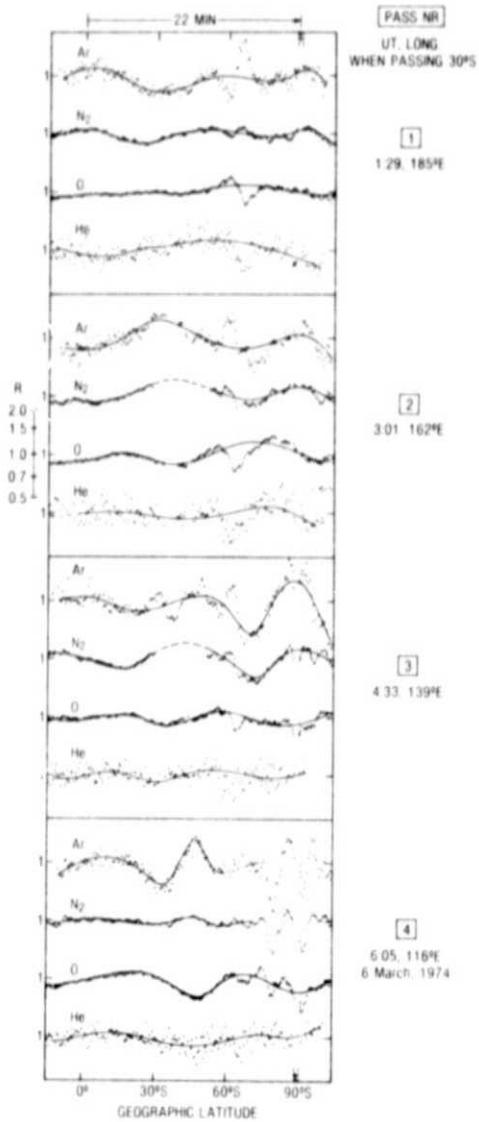

Figure 2: Density ratios R equal to the measured number density data divided by the corresponding density fit value (Figure 1) for Ar, N_2, O and He during four consecutive satellite passes. In order to eliminate variations of global scale occurring during the four considered passes the density fit for each constituent was allowed to vary by the spherical harmonics P_0 and P_1 before computing R for each pass. The ordinate is a logarithmic scale. The latitude region 90° +1° was not sampled by the ESRO 4 (inclination 91°). The $\overline{3}$ hourly index a_p was decreasing from 22 to 7 for passes 1 to 4. The single data points were hand fitted by smoothed curves to emphasize the large scale wave structures.

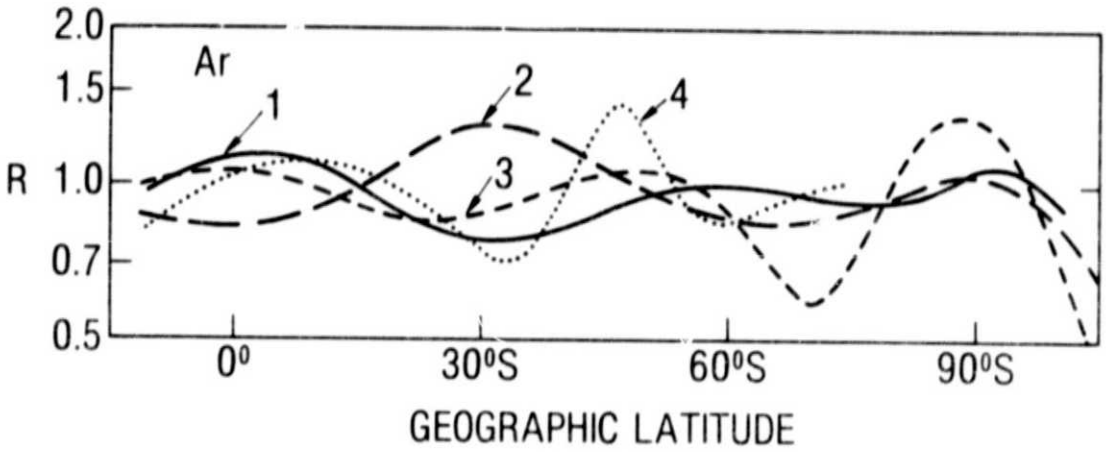

Figure 3: Smoothed density ratios R for argon during four consecutive satellite passes from Figure 2. Notice the time development of the wave structure.

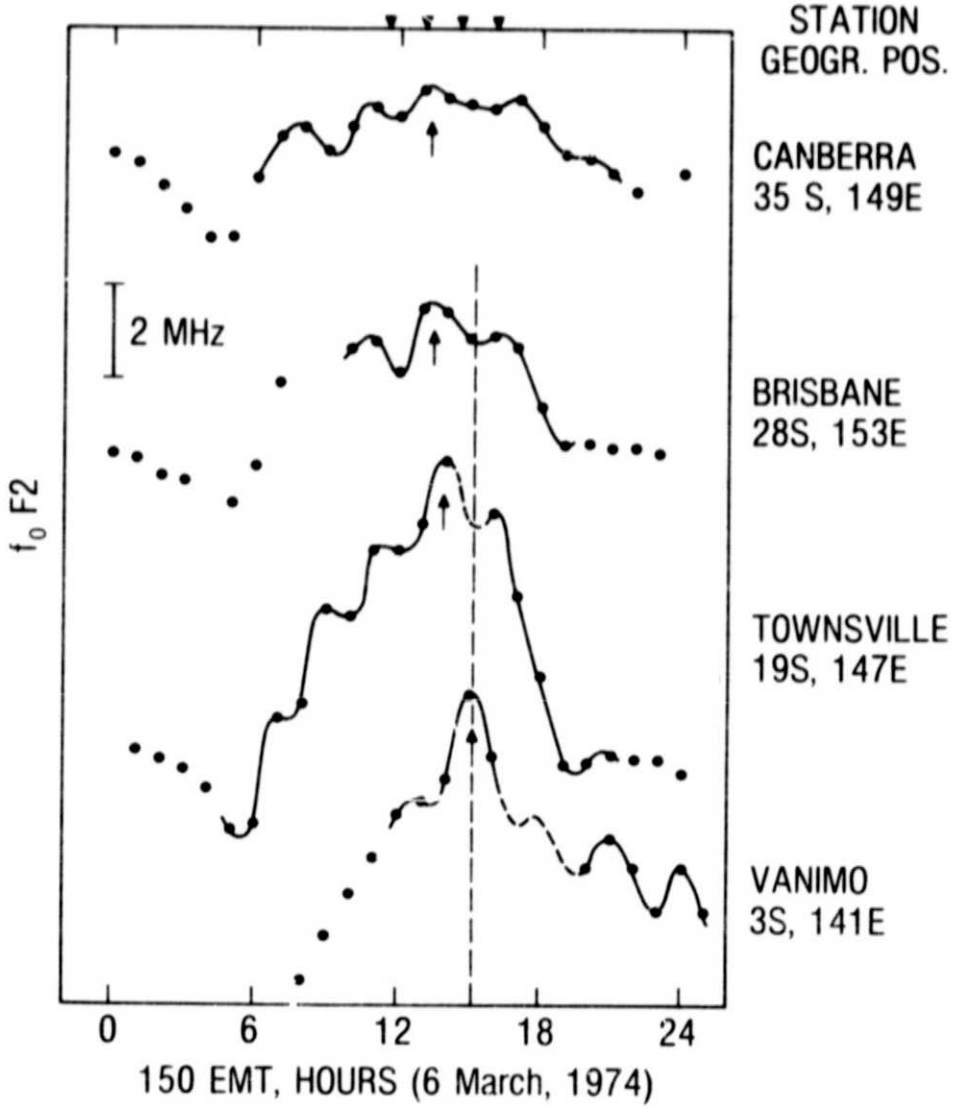

Figure 4. Time variation of the F2 layer critical frequency of four ionosonde stations located at approximately the same geographic longitude which is between the longitudes of ESRO 4 passes 2 and 3 (see Fig. 2). The bar indicates the magnitude of a 2 MHz change in f_0F2. The wave maximum marked by an arrow at each station is believed to be the same maximum migrating from midlatitudes towards the equator. The triangles on top of the figure indicate the times of the four ESRO 4 passes at the geographic latitude of 30°S, (UT=EMT-10 hours). Note, that during the time indicated by the broken line the waves above Brisbane and Vanimo are in antiphase, corresponding to a wavelength of about 5000 km.

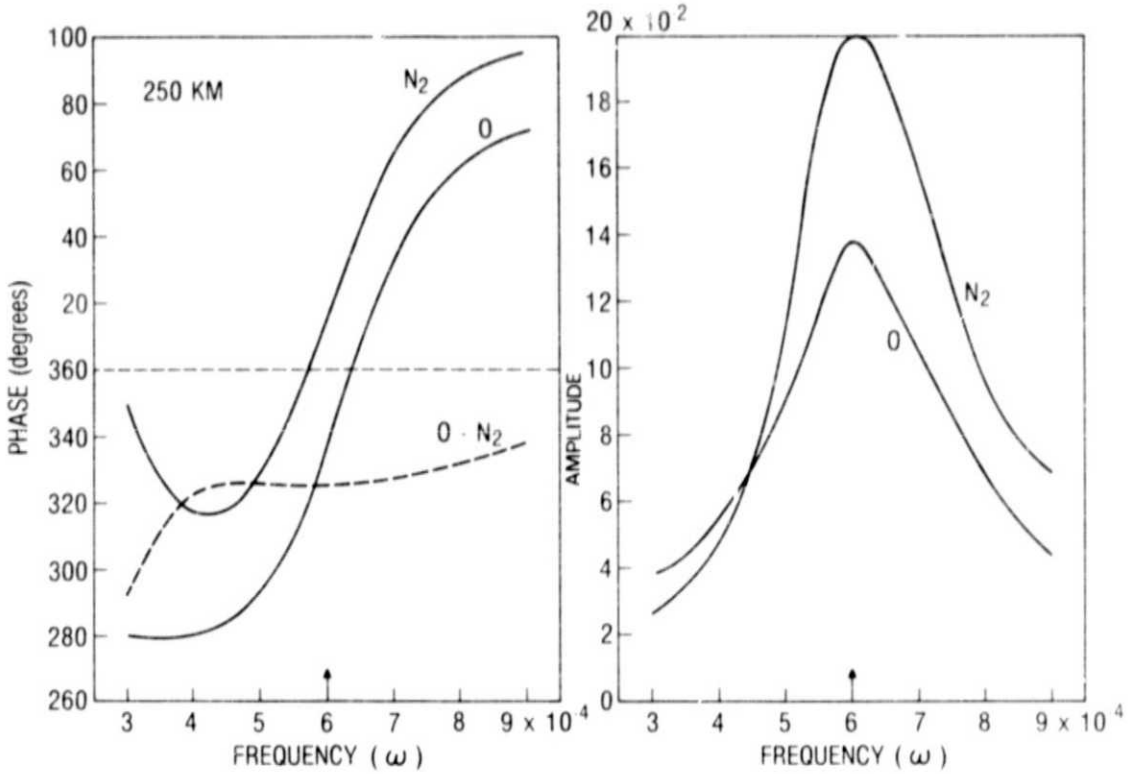

Figure 5: Computed relative amplitudes and phases of N_2 and O for P_8 as a function of frequency ω at 250 km. Also shown is the phase difference between O and N_2. A resonance frequency occurs near $\omega \approx 6 \times 10^{-4}$ sec^{-1} corresponding to a wave period of 2.9 hours.

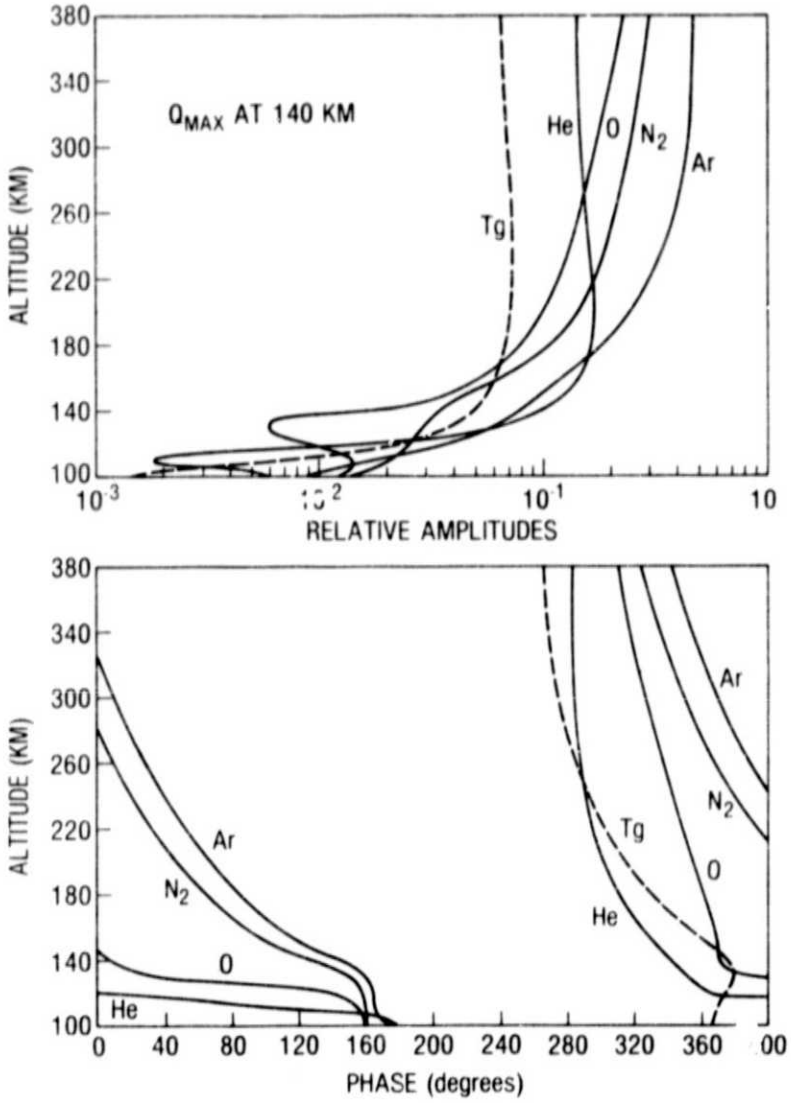

Figure 6: Computed relative amplitudes and phases of Ar, N_2, O, He and Tg as functions of height for P_8 and $\omega = 6 \times 10^{-4}$ sec^{-1}. Note that the temperature is out of phase with N_2 and almost in phase with He.

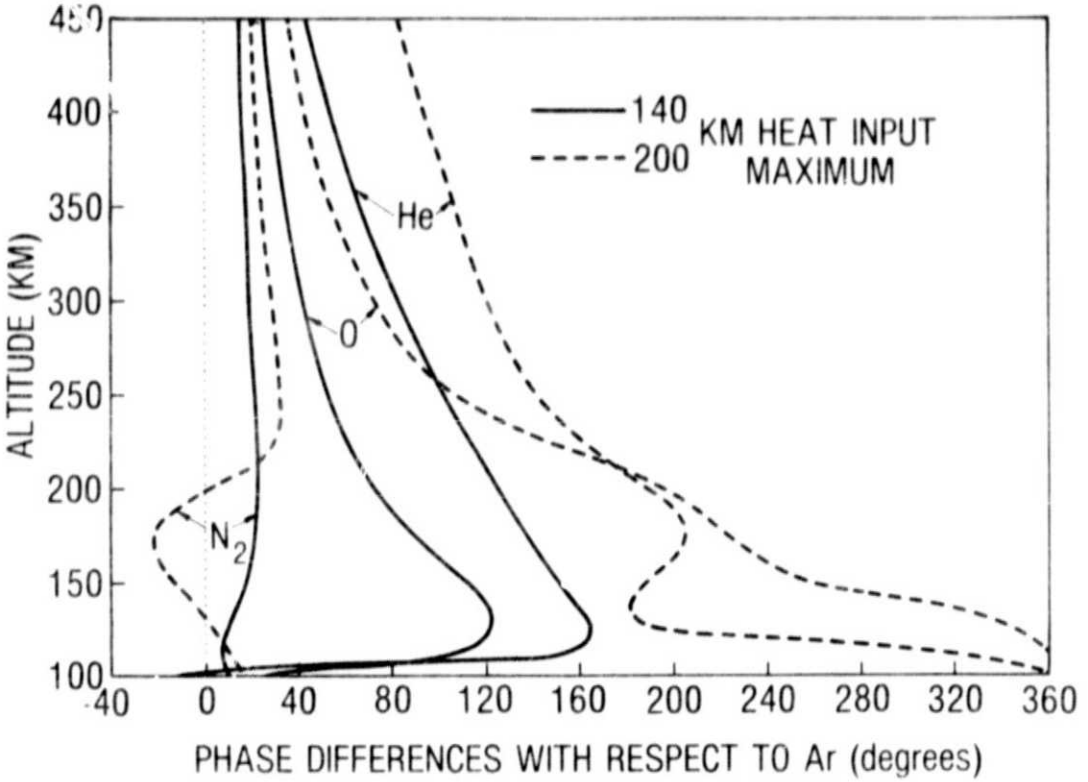

Figure 7: Phase differences for N_2, O and He with regard to Ar computed for two different heat sources, one peaking near 140 km (corresponding to the results in Figures 5 and 6) and another one which peaks near 200 km.